Steel and Composite Structures, *Vol. 32, No. 4 (2019) 497-507*
DOI: https://doi.org/10.12989/scs.2019.32.4.497

Rotational behavior of exposed column bases with different base plate thickness

Yao Cui [*1], Fengzhi Wang [2a], Hao Li [2b] and Satoshi Yamada [3c]

[1] *State Key Laboratory of Coastal and Offshore Engineering, Faculty of Infrastructure Engineering, Dalian University of Technology, No. 2 Linggong-road, Dalian 116024, P.R. China*
[2] *School of Civil Engineering, Faculty of Infrastructure Engineering, Dalian University of Technology, No. 2 Linggong-road, Dalian 116024, P.R. China*
[3] *Institute of Innovative Research, Tokyo Institute of Technology, J2-21, Tokyo Institute of Technology, 4259 Nagatsuda, Midori-ku, Yokohama, Japan*

(*Received January 26, 2019, Revised June 29, 2019, Accepted August 5, 2019*)

Abstract. Exposed column base connections are used in low- to mid-rise steel moment resisting frames. This paper is to investigate the effect of the base plate thickness on the exposed column base connection strength, stiffness, and energy dissipation. Five specimens with different base plate thickness were numerically modelled using ABAQUS software. The numerical model is able to reproduce the key characteristics of the experimental response. Based on the numerical analysis, the critical base plate thickness to identify the base plate and anchor rod yield mechanism is proposed. For the connection with base plate yield mechanism, the resisting moment is carried by the flexural bending of the base plate. Yield lines in the base plate on the tension side and compression side are illustrated, respectively. This type of connection exhibits a relatively large energy dissipation. For the connection with anchor rod yield mechanism, the moment is resisted through a combination of bearing stresses of concrete foundation on the compression side and tensile forces in the anchor rods on the tension side. This type of connection exhibits self-centering behavior and shows higher initial stiffness and bending strength. In addition, the methods to predict the moment resistance of the connection with different yield mechanisms are presented. And the evaluated moment resistances agree well with the values obtained from the FEM model.

Keywords: exposed column base; base plate thickness; anchor rod yield mechanism; base plate yield mechanism; finite element analysis

1. Introduction

Exposed column base connections are commonly used in low- to medium-rise steel moment resisting frames, which comprise a steel base plate welded to the end of the column and anchor rods that connect the base plate to a reinforced concrete foundation beam. A mortar layer is usually placed on between the base plate and the foundation beam. Column base plays a very significant function to transmit active loading from the soil to the structure and return inertia forces from the structure back to the ground. Referring to Fig. 1(a), the loading is carried by stresses in the compression bearing block and tension in the anchor rods. Extensive studies focus primarily on the evaluation of the design strength of column base connections (Dewolf 1982, Thambiratnam and Paramasivam 1986, Astaneh *et al*. 1992, Burda and Itani 1999). Based on these research results, several design guides have been developed, including the American Institute of Steel Construction (AISC) Design Guide 1 (Fisher and Kloiber 2006), AISC Specification for Structural Steel Buildings (AISC 2010b), and AISC Seismic Provisions for Structural Steel Buildings (AISC 2010b) in United States, the ENV1993 Eurocode 3 (ENV, or EuroNorm Vornorm, represents a European prestandard) (CEN 1992) in Europe, and Recommendations for Design of Connections in Steel Structures (AIJ 2006) in Japan.

According to whether the yielding in the base plate occurs before or after the anchor rods yield, the behavior of exposed column base connections is mainly categorized into three types, including rigid base plate connection, flexible base plate connection, and intermediate base plate connection (Astaneh *et al*. 1992). Fig. 1 shows the resistance mechanism of the exposed column base connection with rigid and flexible base plate, respectively. The connection with rigid base plate exhibits pinch and slip behavior, which is dominated by the plastic elongation of anchor rods (Cui *et al*. 2009), as shown in Fig. 1(b). The response of the connection with flexible base plate is controlled by complex interactions between various components, such as the base plate, anchor rods and mortar layer (Kanvinde *et al*. 2013, 2015), as shown in Fig. 1(c).

The effect of the base plate thickness on exposed column base connection strength, stiffness, and energy

*Corresponding author, Ph.D., Associate Professor, E-mail: cuiyao@dlut.edu.cn
[a] Ph.D. Student, E-mail: wang-fz@mail.dlut.edu.cn
[b] Master Student, E-mail: 330520@mail.dlut.edu.cn
[c] Ph.D., Professor, E-mail: yamada.s.ad@m.titech.ac.jp

ISSN: 1229-9367 (Print), 1598-6233 (Online)

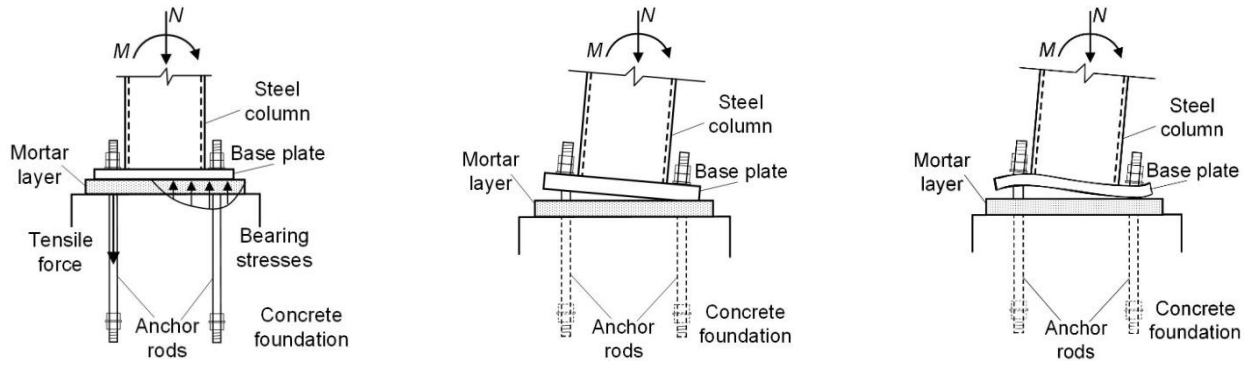

(a) Stress distribution (b) Rigid base plate connection (c) Flexible base plate connection

Fig. 1 Typical exposed column base connections assembly and stress distribution

dissipation have not yet to be systematically investigated. Previous studies focused on the seismic behavior of the exposed column base under a certain scenario, either the connection with rigid base plate or with flexible base plate. Researches conducted by Akiyama (1985), Sato (1987), Cui *et al*. (Cui 2016, Cui *et al*. 2018), and Christopher *et al*. (2016) studied the strength and hysteresis behavior of exposed column base with rigid base plate. While Gomez *et al*. (2009, 2010), Stamatoloulos and Ermopoulos (2011), Khodaie *et al*. (2012), Latour *et al*. (2014), Kanvinde *et al*. (2012, 2015), and Rodas *et al*. (2016) concentrated on the seismic behavior of exposed column base with flexible base plate, including the rotational stiffness, strength and hysteretic model. In addition, Li *et al*. (2016, 2017) conducted extensive finite element analysis to provide an in-depth understanding of the concepts of demountable steel column-baseplate connections. Cassiano *et al*. (2016) discussed the overall structural performance through nonlinear static and dynamic analyses, and Bayat and Zahrai (2017) investigated the effects of semi-rigid connections on the seismic performance of mid-rise steel frames. To systematically study the effect of base plate thickness on the resistance behavior of the exposed column, a series of numerical study are conducted. Based on the analysis results, the critical value of the base plate thickness to identify the yield mechanism is proposed. Moreover, the evaluation of the moment resistance for the connection with different yield mechanisms is established.

2. Prototype model

2.1 Benchmark specimen

A series of quasi-static experiments were conducted by Cui *et al*. (Cui 2016, Cui *et al*. 2018) to study the shear behavior and seismic behavior of exposed column base connections with rigid base plate. The specimens were tested at approximately two-thirds scale and were designed to simulate interior column base connections in low-rise steel structures according to the associated provisions of *Recommendation for Design of Connections in Steel Structures* (AIJ 2006). Moreover, a typical configuration of the exposed column base connection comprises a steel base plate welded to the end of the column and anchor rods that connect the base plate to reinforced concrete (RC) foundation beam. The anchor rods are embedded in the RC foundation beam in advance, and then the nut would be hand tighten after the connection is assembled. The force applied to the anchor rods is relatively small so that it is not considered in the numerical model.

Fig. 2 shows the basic dimensions of the specimen,

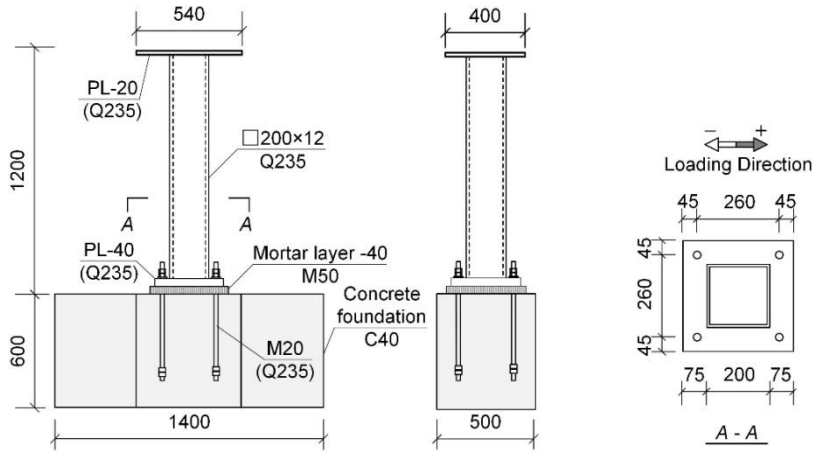

Fig. 2 Test specimen (unit: mm)

Fig. 3 Test setup

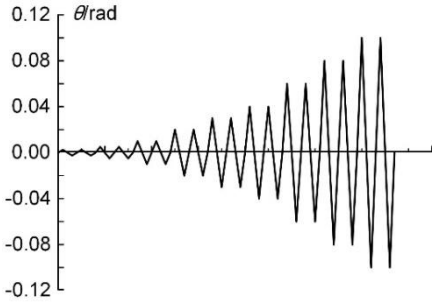

Fig. 4 Loading history

comprising a square-tube cross-section column (200 mm × 12 mm), a square rigid base plate (350 mm × 350 mm × 40 mm), anchor rods, and an RC foundation beam. To ensure the anchor rods yielding and the base plate remain elastic throughout the test program, the foundation beam was designed strong enough so that a cone-like failure of concrete would not occur and a 40-mm-thick base plate was used. By controlling the full plastic moment ratio of the column is 1.2 times that of the corresponding exposed column base connection, a relatively strong column was used to make sure that the damage concentrated on the connection during cyclic loading before unrecoverable plastic deformation occurred in the column.

Specimen '4RM' was designed as the prototype specimen, which was subjected to a constant vertical force of 540 kN (axial force ratio of 0.2). The test setup was photographically illustrated in Fig. 3. The column top was clamped to the horizontal hydraulic jack and the vertical hydraulic jack at the same time. During the loading, the axial force kept constant and a displacement-controlled cyclic load was applied quasi-statically in the horizontal direction. The loading history was shown in Fig. 4. The loading rotation angles of 0.005, 0.01, 0.02, 0.03, 0.04, 0.06, 0.08, and 0.1 rad were adopted, and two cycles were performed at each loading level.

2.2 FEM model

The general finite element software ABAQUS (2014) was used to investigate the seismic behavior of the specimen. As the geometrical dimensions of Specimen '4RM' was the same as that of Specimen '4RM-40', which

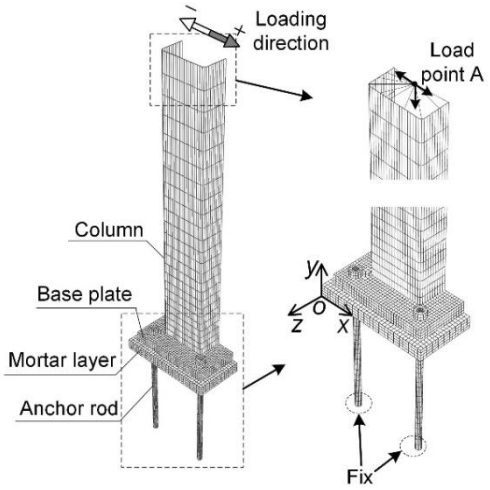

Fig. 5 Boundary and loading condition

would be studied in the subsequent part. Therefore, Specimen '4RM' was selected to calibrate the numerical model. As observed from the test, the damage was concentrated on the anchor rods without failure of the RC foundation beam occurred. The RC foundation is not simulated explicitly in the numerical model for simplicity. As shown in Fig. 5, half of the specimen is modeled by considering the symmetry and boundary conditions. The four-node quadrilateral surface element (S4R) was used for the column, and the three-dimensional eight-node element with reduced integration (C3D8R) was used for the base plate, anchor rod, and mortar layer. The shell-solid coupling was used to connect the column and base plate by considering the compatibility between the difference in DOF at a node in the shell and 3D solid elements.

The finite element material properties were defined according to the experimental results as previously mentioned (Cui *et al*. 2018). The isotropic hardening model with Young's modulus $E = 2.05\times10^5$ MPa and Poisson's ratio of 0.3 was adopted to simulate the column, base plate, and anchor rods. Both the yield strength and ultimate strength of the column and the base plate were f_y = 373 MPa, f_u = 486 MPa, respectively. The yield strength of 279.7 MPa and ultimate strength of 500.3 MPa were adopted to simulate the anchor rods. The Von Mises yield criterion was used for the yield criterion of material. The damage plasticity model was adopted with the compression stress of 50 MPa for mortar layer, dilation angle of 36.31°, eccentricity of 0.1, f_{bo}/f_{co} = 1.13, K = 0.667, viscosity parameter of 0.0001, Young's modulus E of 4.94×10^4 MPa and Poisson ratio of 0.2.

As shown in Fig. 6, the interaction between each part of the specimens, such as the contact between steel column and base plate, anchor rods and base plate, anchor rods and mortar layer, were modeled. The friction coefficient of contact interaction between the bottom of the base plate and the top of the mortar layer is 0.55 (Nagae *et al*. 2006). The interface pairs, such as the contact between anchor rods and hole of base plate, is defined as frictionless contact.

Considering the symmetry, a symmetrical boundary condition was imposed on the symmetry plane XOY as

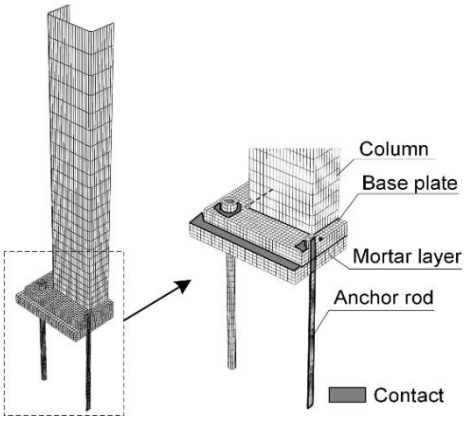

Fig. 6 Interaction property

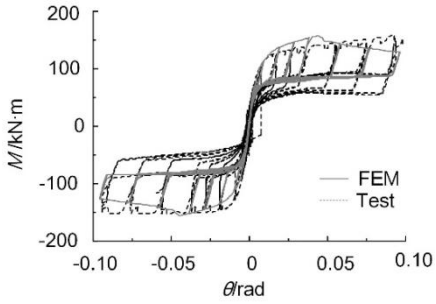

Fig. 7 Comparison of the numerical and experimental hysteresis curves

shown in Fig. 5, both the translation of the Z-axis and the rotation around the X-axis and Y-axis were restrained. For the convenience of simplification, the nodes of the bottom of the anchor rods and mortar layer were fixed. The displacement in the X-axis and Z-axis of the anchor rods within the concrete were restrained to simulate the interaction property between the anchor rods and concrete.

To simulate the behavior of the column subjected to the lateral load under a constant vertical axial force, the reference point A was set on the top of the column. Compressive load of 270 kN (axial load ratio of 0.2), was applied on the reference point. A displacement-controlled lateral load was adopted, the loading process was consistent with that of the tests, as shown in Fig. 4.

2.3 Calibration of FEM model

In Japan, yielding is allowed for the column bases with anchor rod yield mechanism under large earthquakes, if ductile anchor rods are to be used. With reference to the experimental results in the previous study (Cui 2016, Cui *et al*. 2018), the hot-rolled anchor rods satisfies this condition and exhibits excellent ductility, which enables the exposed column base to have large plastic deformation capability. As mentioned previously, the connection is not simulated comprehensively in the numerical model for simplicity. For instance, the bonding behavior between the anchor rods and RC foundation beam is neglected, which may affect the behavior of the connection in reverse. Fig. 7 compared the hysteresis curves of Specimen '4RM' obtained from the experimental and numerical studies. The horizontal axis represents the rotation angle of the column top and the vertical axis represents the resisting moment at the base plate. It is notable that the pinch and slip behavior due to the elongation of anchor rods could be reasonably traced by the numerical model. The rotation angle corresponding to the maximum moment resistance in the numerical model is different from that in the test. This may be attributed to the failure of considering the bonding behavior and other uncertain factors, which requires further investigation.

The failure mode of Specimen '4RM' as the column top rotation angle is 0.1 rad obtained from the experimental and numerical studies are shown in Fig. 8. In the test, it is observed that the tension load resisted by the anchor rods on the tension side are balanced with the bearing resistance between the base plate and mortar layer. Moreover, the rotation point is located at the anchor rods on the compression side, as shown in Fig. 8(a). The same deformation is represented by the numerical model shown in Fig. 8(b). In addition, the differences in the yield and maximum moment resistance obtained from numerical and test results are around 9% and 2.7%, respectively.

It is particularly noticeable that the resistance mechanism and yield moment resistance of the exposed column base connections with different base plate thickness are the focuses of this paper. Taking the small rotation angle of the column top into account, less than 0.03 rad, both the failure mode and moment resistance of the connection can be reasonably traced by the numerical model. Therefore, the numerical model illustrated in this section is adopted for further parametric studies.

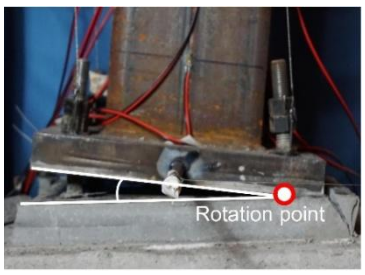

(a) Test result

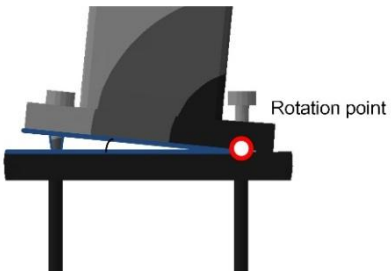

(b) FEM result

Fig. 8 Failure mode of FEM and test specimen

3. Parametric studies

To investigate the effect of base plate thickness on the seismic behavior of exposed column base connections, the parametric studies using the above mentioned numerical model were conducted. The studied parameter is the thickness of the base plate. And the thickness of the base plate is varied from 10 mm to 40 mm. The naming rule for the specimens is as follows, for instance, '4RM-10' represents that the specimen with the base plate thickness of 10mm. In the following discussion, '4RM-40' is the same as above mentioned numerical model '4RM'.

3.1 Moment-rotation relationships

Fig. 9 shows the moment-rotation curve for all five specimens under cyclic loading obtained from numerical analysis. The horizontal axis represents the rotation angle of the column top, and the vertical axis represents the resisting moment at the bottom of the base plate. The P-Δ effect is considered in the resisting moment. At the early loading stage, the moment produced by the horizontal load is balanced by the axial force. As shown in Fig. 9, the hysteresis curves of specimens tend to pinch as the thickness of base plate increased. As the thickness of the base plate is increased, the hysteresis curve trend to flag-shape and the residual rotation is nearly zero. The specimen shows self-centering behavior.

Table 1 summarizes the initial stiffness (K_0), the maximum moment resistance (M_u), and the equivalent viscous-damping ratio (h_e) at the 0.1 rad rotation angle observed from the parametric study. The initial stiffness of the specimen is defined as the secant slope of the hysteresis curve when the column top rotation angle is 0.5%. The moment resistance corresponding to the peak point of the hysteresis curves is defined as the maximum strength (M_u). The equivalent viscous-damping ratio is adopted herein as the normalization strategy to determine the capacity of energy dissipation ideally for each specimen. The triangular area of the force and displacement diagram at each drift amplitude serves as the basis for normalization. It is obvious that the greater the equivalent viscous-damping ratio, the greater the energy dissipated by the specimen, which would exhibit excellent seismic behavior.

Table 1 FEM results

	Initial stiffness K_0/kN·m/rad	Maximum moment M_u/kN·m	Equivalent viscous-damping ratio h_e
4RM-10	10929	98.60	0.738
4RM-15	11278	115.64	0.732
4RM-20	12962	128.09	0.389
4RM-30	16263	146.01	0.349
4RM-40	17827	168.51	0.295

As shown in Table 1, a negligible difference (within 5%) of initial stiffness and the equivalent viscous-damping ratio is notable between Specimens '4RM-10' and '4RM-15'. It is speculated to be because the failure mode for the specimens is the same. Furthermore, the initial stiffness and the equivalent viscous-damping ratio are dominated by the failure mode of the exposed column base connections. For Specimen '4RM-15', the maximum moment strength increases 17% compared with that of Specimen '4RM-10'. As the thickness of the base plate increased, the improvement in the initial stiffness and maximum moment strength varied from 20% to 60% and 30% to 70%, respectively. But the equivalent damping ratio is reduced from 50% to 40%. This indicates that the base plate plays a key role in terms of the energy dissipation of the exposed column base connections, which will be discussed in the following section. Specimen '4RM-40' shows the largest improvement on both the initial stiffness and maximum moment strength, but the largest reduction on the equivalent

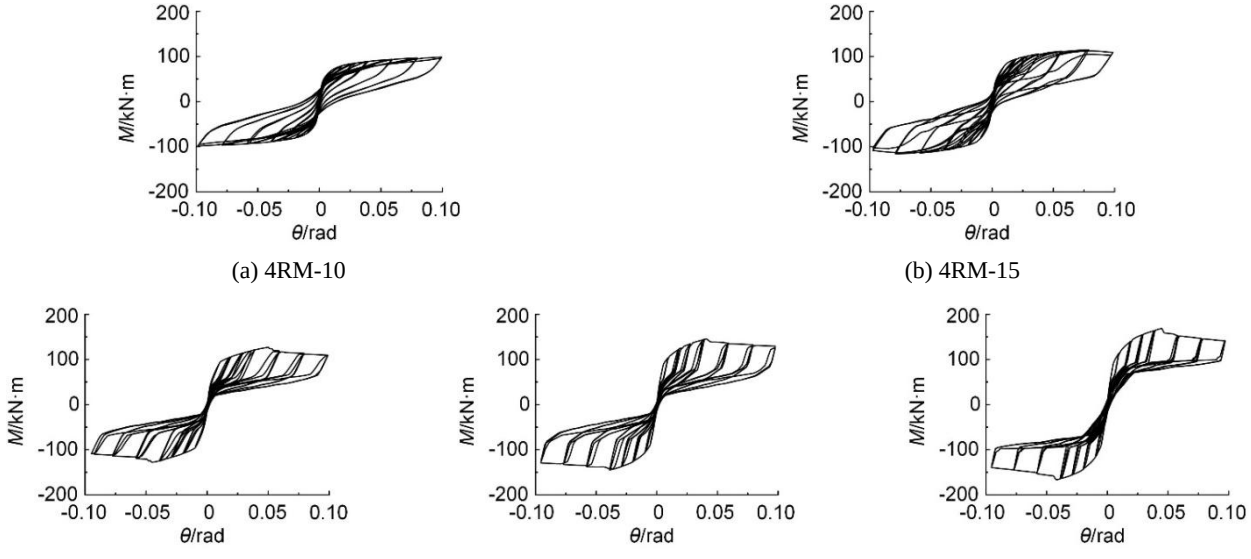

(a) 4RM-10 (b) 4RM-15

(c) 4RM-20 (d) 4RM-30 (e) 4RM-40

Fig. 9 Moment-rotation relationships

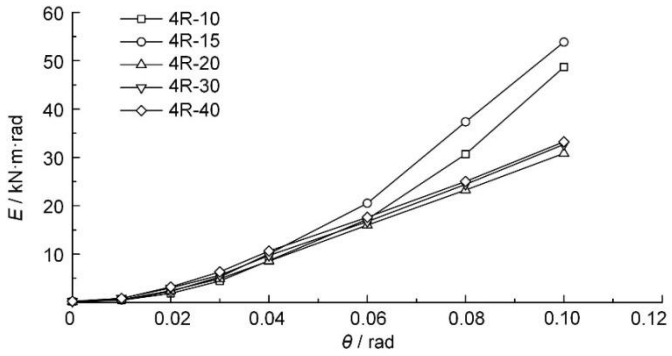

Fig. 10 Cumulative energy dissipation of each loading cycle

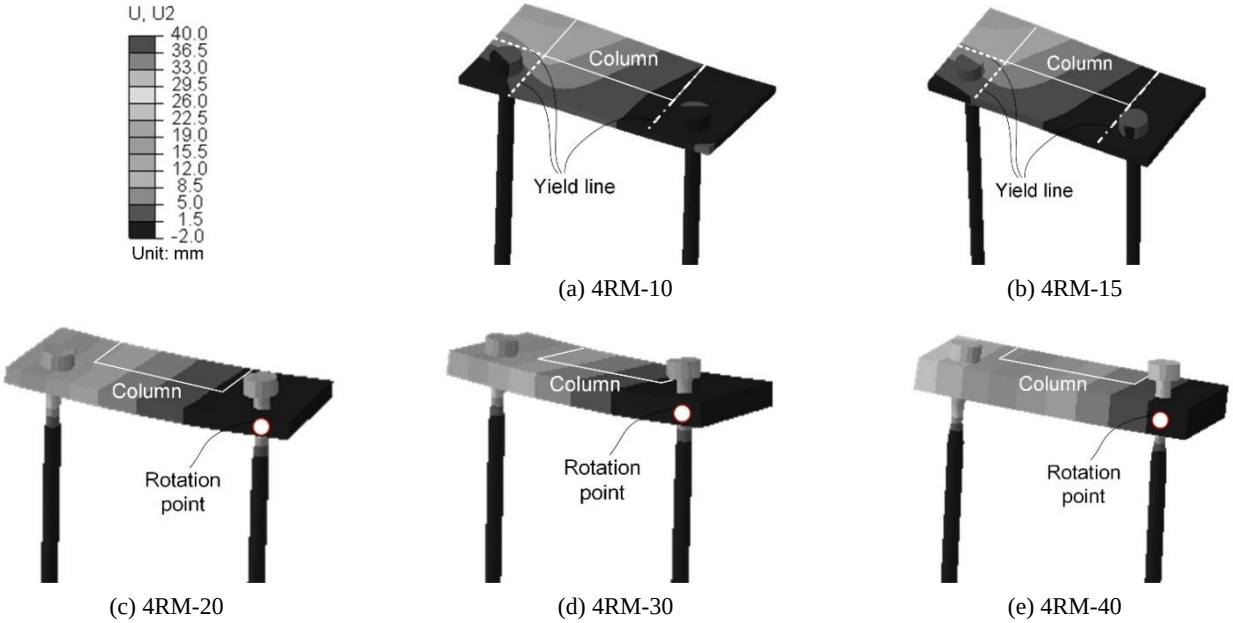

(a) 4RM-10 (b) 4RM-15

(c) 4RM-20 (d) 4RM-30 (e) 4RM-40

Fig. 11 Failure modes of specimens with different base plate thickness

viscous-damping ratio.

It is noted that specimens with a thicker base plate, t_{bp} > 15 mm, shows larger initial stiffness and maximum moment strength. Oppositely, the specimens with thinner base plate, $t_{bp} \leq 15$ mm, shows smaller initial stiffness and maximum moment strength, but larger energy dissipation capacity.

Cumulative energy dissipations of each loading cycle for each specimen are illustrated in Fig. 10. The vertical-horizontal axis represents the dissipated energy, derived from the area of the moment-rotation curve at the end of each rotation angle of the column top increment until the column rotation angle is 0.1 rad. It is obvious that the energy dissipation of specimens with a flexible base plate ($t_{bp} \leq 15$ mm) is significantly greater than that of specimens with a rigid base plate ($t_{bp} > 15$ mm). The dissipated energy increased by around 2 times as the base plate thickness decreases from 40 mm to 15 mm as the column rotation angle is 0.1 rad. It is noted that the value of cumulative dissipated energy is the same during the loading when the thickness of the base plate is greater than 15 mm. Given that previous discussion on the equivalent viscous-damping ratio demonstrates a similar conclusion, exposed column bases with a flexible base plate present higher energy dissipation capacity. This may be attributed to the high ductility of the flexible base plate due to its bending. While the energy dissipation capacity of the exposed column bases with a rigid base plate depends on the ductility of the anchor rods.

3.2 Failure mechanisms

Fig. 11 shows the failure modes of the exposed column base connections with different base plate thickness at 0.1 rad column rotation. The connections are grouped into two categories: flexible base plate connection and rigid base plate connection. When the base plate thickness is less than or equal to 15 mm (Specimens ‘4RM-10’ and ‘4RM-15’), bending of the base plate occurs and the deformation is concentrated on the distribution between anchor rods. The yield lines in the base plate are outlined in Figs. 11(a) and (b), which will be discussed in the subsequent section. It can be seen that the anchor rods do not yield on the tension side of the connection. Therefore, the failure mode of a flexible base plate connection is controlled by the flexure of the base plate, designated as base plate yield mechanism.

The key feature is that these two specimens show relatively large energy dissipation.

When the base plate thickness is greater than 15 mm (Specimens '4RM-20', '4RM-30' and '4RM-40'), the base plate shows the behavior of rigid body rotation and the anchor rod is elongated as the base plate rotates as shown in Figs. 11(c)-(e). Therefore, the failure mode of a rigid base plate connection is determined by elongation of anchor rods on the tension side, designated as anchor rod yield mechanism. The connection exhibits self-centering behavior and shows higher initial stiffness and bending strength.

4. Evaluation of moment resistance

4.1 Resistance mechanism

As mentioned in the above, two failure modes are possible corresponding to the thickness of base plate: (1) base plate yield mechanism (Figs. 11(a)-(b)) and (2) anchor rod yield mechanism (Figs. 11(c)-(e)). Fig. 11(a) shows the deformation of the connection with base plate yield mechanism, the base plate yield on the tension side due to the tension in the anchor rods and the base plate yield on the compression side due to the upward bearing stress. The applied loading is resisted solely through the flexural yielding of the base plate, determined by the yield lines of in the base plate on both the tension and compression sides of the connection. Fig. 11(e) shows the deformation of the connection with anchor rod yield mechanism, the anchor rods yield on the tension side caused by the rotation of the base plate. The loading is resisted through a combination of tensile forces in the anchor rods and bearing stresses on the compression side of the connection.

It is necessary to clarify the distribution of yield lines in the base plate of the connection with the base plate yield mechanism. Given all of the above, assumed force and yield lines distribution of the connection is indicated schematically in Fig. 12. On the tension side, the base plate tends to uplift and is constrained by the downward force T_{ya} of the anchor rods. It is apparent that the closer to the steel column edge, the larger the deformation of the base plate. On the compression side, the base plate contacts with the mortar layer. The bearing stress between the base plate and the mortar layer is observed.

Consequently, the yield lines in the base plate on the tension side of the connection are straight lines from the steel column edge to the base plate edge, the bending of the base plate in the area between the column edges is negligible. The length of a single yield line is denoted as *l*. This is indicated schematically in Fig. 12(b). The yield line in the base plate on the compression side of the connection is parallel to the column edge. The length of the yield line is the width of the base plate, denoted as *B*, as shown in Fig. 12(b). Hereafter, the critical base plate thickness is proposed to distinguish these two yield mechanisms based on the distribution of yield lines.

4.1.1 Base plate yield on the tension side

It is assumed that the yielding area of the base plate on both the tension and compression sides of the connection is regarded as a cantilever fixed to the column edge. On the tension side, the mechanical model is illustrated in Fig. 12(a). The bending strength of the tensile force T_{ya} in the anchor rods to the steel column edge is calculated as

$$M_{ab} = T_{ya}(l - s) \tag{1}$$

where T_{ya} = yield tensile force of the anchor rod, estimated as $f_{y,ab}A_e$; $f_{y,ab}$ = yield strength of the anchor rod; A_e = effective area of the anchor rod; l = base plate edge distance; s = anchor rod edge distance.

Referring to Fig. 12(b), the four yield lines in the base plate on the tension side are symmetrical in the connection where a symmetrical anchor rod pattern in both directions is used. The full plastic moment resistance of a single yield line *l* is then calculated as

$$M_{bp,t} = \frac{1}{4} l t_{bp,t}^2 f_{y,bp} \tag{2}$$

where $f_{y,bp}$ = yield strength of the base plate; $t_{bp,t}$ = thickness of the base plate on the tension side.

Assuming that yielding of the base plate on the tension side and yielding of the anchor rods occur at the same time. In particular, there are two yield lines corresponding to yielding of an anchor rod. Thus, the required thickness of the base plate on the tension side is

$$M_{bp,t}^2 = 2A_e \frac{l - s}{l} \frac{f_{y,ab}}{f_{y,bp}} \tag{3}$$

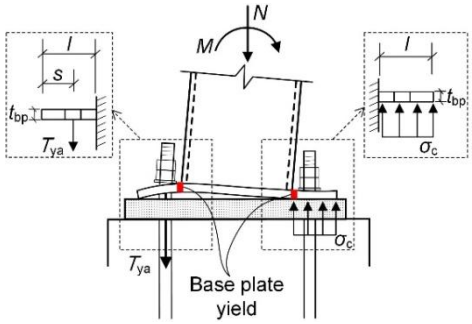

(a) Force distribution

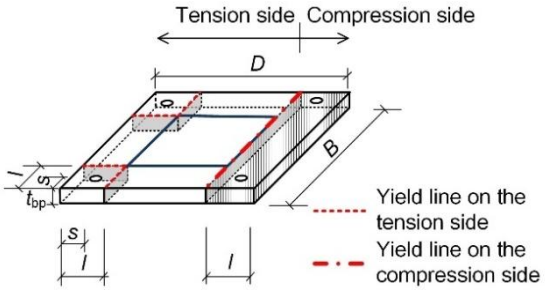

(b) Yield lines distribution

Fig. 12 Assumed force and yield lines distribution of the connection with base plate yield mechanism

4.1.2 Base plate yield on the compression side

On the compression side of the connection, rectangular stress is distributed over an area that is the width of the base plate B by the base plate edge distance l as shown in Fig. 12(a). The bending strength of the base plate under the upward bearing stress to the steel column edge is calculated as

$$M_{\mathrm{b}} = \frac{1}{2}\sigma_{\mathrm{c}} l^2 \tag{4}$$

where $\sigma_{\mathrm{c}} = f_{\mathrm{c}}B$; f_{c} = bearing stress between the base plate and mortar layer; B = width of the base plate.

From Fig. 12(b), the full plastic moment resistance of the yield line in the base plate on the compression side B is calculated as

$$M_{\mathrm{bp,c}} = \frac{1}{4} B t_{\mathrm{bp,c}}^2 f_{\mathrm{y,bp}} \tag{5}$$

where $t_{\mathrm{bp,c}}$ = thickness of the base plate on the compression side.

To characterize the required thickness of the base plate on the compression side, Eqs. (4) and (5) should coincide, therefore the required thickness of the base plate on the compression side is

$$t_{\mathrm{bp,c}}^2 = 2l^2 \frac{f_c}{f_{\mathrm{y,bp}}} \tag{6}$$

4.1.3 Critical baseplate thickness

The critical thickness of the base plate is, therefore, the minimum value of the required base plate thickness on the tension side, $t_{\mathrm{bp},t}$, and that on the compression side, $t_{\mathrm{bp,c}}$, that is

$$t_{\mathrm{bp}} = \min\left(t_{\mathrm{bp,t}}, t_{\mathrm{bp,c}}\right) \tag{7}$$

The critical value of the base plate thickness is dependent on the layout of the connection, the bearing stress, and the yield strength of the base plate. For the specimens considered in this paper, the bending strength of the downward force in the anchor rods to the steel column edge is 2.64 kN·m. Then the required thickness of the base plate on the tension side is 13.70 mm, obtained by solving Eq. (3). The bending strength of the base plate under the upward bearing stress to the steel column edge is 49.22 kN·m. According to Eq. (6), the required thickness of the base plate on the compression side is 38.83 mm. Consequently, the critical value of the base plate thickness is 13.7 mm, which is consistent with the value (15 mm) observed from the previous numerical study.

4.2 Evaluation of moment resistance

4.2.1 Base plate yield mechanism

As discussed previously, the moment resistance of the exposed column base is determined by the yield mechanism. Fig. 13 illustrates the geometrical relationship and two deformation modes of the connection. For the connection with base plate yield mechanism Fig. 13(b), the base plate itself is subjected to bending on both the tension and compression sides of the connection. As a result, the entire moment may be resisted exclusively through the development of the flexural yielding of the base plate on the tension and compression sides, $M_{\mathrm{bp,t}}$ and $M_{\mathrm{bp,c}}$, in addition to the applied axial load, M_{N}. Applying the principle of virtual work, the work done by external forces is equal to that done by the flexural yielding of the base plate, that is

$$M_{y.B} \cdot \theta = M_{\mathrm{bp,t}}^{\mathrm{total}} \cdot \theta_t + M_{\mathrm{bp,c}} \cdot \theta_c + M_N \cdot \theta \tag{8}$$

$$M_N = N \cdot \frac{d}{2} \cdot \theta \tag{9}$$

where $M_{\mathrm{y,B}}$ = yield moment resistance of the connection with base plate yield mechanism; $M_{\mathrm{bp,t}}^{\mathrm{total}}$ = total full plastic moment resistance of yield lines in the base plate on the tension side; θ_{t} = rotation of the base plate on the tension side; $M_{\mathrm{bp,c}}$ = full plastic moment resistance of yield lines in the base plate on the compression side; θ_{c} = rotation of the base plate on the compression side; M_{N} = moment resistance produced by applied axial load; N = applied axial load; d = depth of column section; θ = rotation of the column.

As shown in Fig. 13(b), considering the deformation compatibility, the relationship between the rotation of different parts of the connection is as follows

$$\theta = \theta_{\mathrm{c}} \tag{10}$$

$$\frac{\theta_{\mathrm{t}}}{\theta} = 1 + \frac{d}{l - s} \tag{11}$$

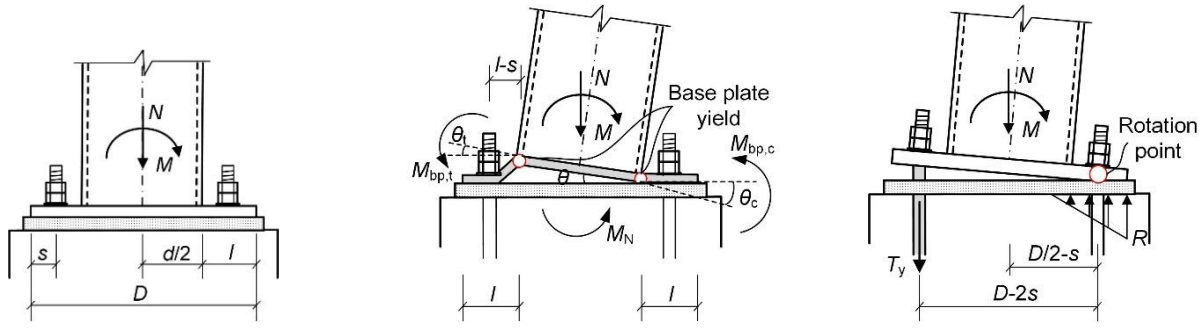

(a) Geometrical relationship (b) Base plate yield mechanism (c) Anchor rod yield mechanism

Fig. 13 Deformation modes of the exposed column base connection

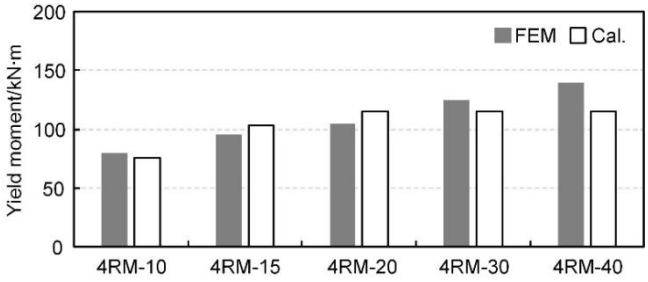

Fig. 14 Comparison of yield moment resistance determined from FEM and method

Substituting Eqs. (2), (5) and (9)-(11) into Eq. (8) gives the yield moment resistance of the connection, $M_{y,B}$, as outlined in Eq. (12).

$$M_{y.B} = lt_{\mathrm{bp}}^2 f_{y,\mathrm{bp}}\left(1+\frac{d}{1-s}\right)+\frac{1}{4}Bt_{\mathrm{bp}}^2 f_{y,\mathrm{bp}}+N\frac{d}{2} \quad (12)$$

4.2.2 Anchor rod yield mechanism

For the connection with anchor rod yield mechanism Fig. 13(c), the moment at the connection is resisted by the development of a force couple between bearing stresses under the base plate and tension force in the anchor rods. The predicted moment resistance of the connection has been summarized (Cui 2016, Fisher and Kloiber 2006, AIJ 2006), which assumes that the position of the rotation point is located at the anchor rods on the compression side when the connection yield. Triangular compressive bearing stress is distributed under the base plate and the action point is located at the anchor rods on the compression side. The yield moment resistance of the connection is then calculated as

$$M_{y.A} = T_y(D-2s)+N(D/2-s) \quad (13)$$

where T_y = total yield tensile force of anchor rods on the tension side, estimated as $nf_{y,ab}A_e$; n = number of the anchor rods in tension; D = length of the base plate.

4.2.3 Verification

Following the methodology described in the previous section, the comparison between FEM and calculated results of yield moment resistance are listed in Fig. 14. For Specimens '4RM-10' and '4RM-15', designated as base plate yield mechanism, the difference between evaluated and FEM results are within 10%. For Specimens '4RM-20', '4RM-30' and '4RM-40', designated as anchor rod yield mechanism, the evaluation underestimates the yield moment resistance and the difference between evaluated and FEM results are less than 20%. This demonstrates that the proposed deformation mechanism of the connection with base plate yield mechanism is in good agreement with the FEM results. The evaluation of the yield moment resistance is reliable and acceptable.

5. Conclusions

In this paper, finite element models are developed to simulate the seismic behavior of the exposed column base connection with different base plate thickness. For exposed column base connections with a four-rod layout, the critical value of the base plate thickness to identify the base plate yield or anchor rod yield mechanism is proposed. The yield lines in the base plate of the connection with base plate yield mechanism are addressed based on the bending of the base plate. This paper presents methods to characterize the moment resistance of the connection with different yield mechanisms. The following key conclusions emerge from this study:

(1) The failure mode of the exposed column base connection is dependent on the thickness of the base plate. When the thickness of the base plate is less than or equal to the critical value, the connection is designated as base plate yield mechanism. When the thickness of the base plate is greater than the critical value, the connection is designated as anchor rod yield mechanism.

(2) For the connection with base plate yield mechanism, the base plate itself is subjected to bending on both the tension and compression sides of the connection. The yield lines in the base plate on the tension side of the connection are straight lines from the steel column edge to the base plate edge. On the compression side of the connection, yield lines form parallel to the column edge. The critical value of the base plate thickness to distinguish the two yield mechanisms is determined based on those yield lines. The key feature of this connection is large energy dissipation.

(3) For the connection with anchor rod yield mechanism, tension is developed in the anchor rods as a result of the rigid body rotation of the base plate. The position of the rotation point is assumed to locate at the anchor rods on the compression side when the connection yield. This connection exhibits self-centering behavior and shows higher initial stiffness and bending strength.

(4) The methods to characterize the moment resistance of the exposed column base connection with different yield mechanisms subjected to a combination of flexural and axial loads are presented. For the connection with base plate yield mechanism, the entire moment may be resisted solely through the flexural yielding of the base plate. While for the connection with anchor rod yield mechanism, the applied moment is resisted

through a combination of bearing stresses on the compression side and tensile forces in the anchor rods. Overall, the methods predict the FEM results observed yield moment resistance with reasonable accuracy.

Acknowledgments

This work was supported by the National Science Fund of China (51208076, 51678106) and the Collaborative Research Project of Laboratory for Materials and Structures, Institute of Innovative Research, Tokyo Institute of Technology. Their financial support is highly appreciated.

References

ABAQUS analysis user's guide (2014) (version 6.14), ABAQUS Inc, USA.

Akiyama, H. (1985), "The seismic design of steel bone column base", Tokyo, Japan. [In Japanese]

American Institute of Steel Construction (AISC) (2010a), Specification for Structural Steel Buildings, ANSI/AISC 360-10, Chicago, IL, USA.

American Institute of Steel Construction (AISC) (2010b), Seismic Provisions for Structural Steel Buildings, ANSI/AISC 341-10, Chicago, IL, USA.

Architectural Institute of Japan (AIJ) (2006), Recommendations for Design of Connections in Steel Structures, Tokyo, Japan.

Astaneh, A., Bergsma, G. and Shen, J.H. (1992), "Behavior and design of base plates for gravity, wind and seismic loads", *Proceedings of the National Steel Construction Conference*, AISC, Chicago, IL, USA.

Bayat, M. and Zahrai, S.M. (2017), "Seismic performance of mid-rise steel frames with semi-rigid connections having different moment capacity", *Steel Compos. Struct., Int. J.*, **25**(1), 1-17. https://doi.org/10.12989/scs.2017.25.1.001

Burda, J.J. and Itani, A.M. (1999), "Studies of seismic behavior of steel base plates", Rep. No. CCEER 99-7; Center for Civil Engineering Earthquake Research, University of Nevada, Reno, NV, USA.

Cassiano, D., Aniello, M.D., Rebelo, C., Landolfo, R. and Silva, L.S. (2016), "Influence of seismic design rules on the robustness of steel moment resisting frames", *Steel Compos. Struct., Int. J.*, **21**(3), 479-500. https://doi.org/10.12989/scs.2016.21.3.479

Christopher, A.T., Tara, H., Philipp, R.G. and John, F.S. (2016), "Effects of detailing on the cyclic behavior of steel baseplate connections designed to promote anchor yielding", *J. Struct. Eng.*, **142**(2), 04015117. https://doi.org/10.1061/(ASCE)ST.1943-541X.0001361

Cui, Y. (2016), "Shear behavior of exposed column base connections", *Steel Compos. Struct., Int. J.*, **21**(2), 357-371. https://doi.org/10.12989/scs.2016.21.2.357

Cui, Y., Nagae, T. and Nakashima, M. (2009), "Hysteretic behavior and strength capacity of shallowly embedded steel column bases", *J. Struct. Eng.*, **135**(10), 1231-1238. https://doi.org/10.1061/(ASCE)ST.1943-541X.0000056

Cui, Y., Liu, H., Li, H. and Wang, J.Q. (2018), "Experimental study on seismic behavior of exposed steel column base", *J. Build. Struct.*, **39**(7), 115-122. https://doi.org/10.14006/j.jzjgxb.2018.07.013

DeWolf, J.T. (1982), "Column base plates", *Struct. Eng. Practice*, **1**(1), 39-51.

European Committee for Standardization (CEN) (1992), ENV Eurocode 3: Design of Steel Structures, Brussels, Belgium.

Fisher, J.M. and Kloiber, L.A. (2006), Design guide 1: Base Plate and Anchor Rod Design, (2nd Edition), AISC, Chicago, IL, USA.

Gomez, I., Kanvinde, A., Smith, C. and Deierlein, G. (2009), "Shear transfer in exposed column base plates", AISC, Chicago, USA.

Gomez, I., Kanvinde, A. and Deierlein, G. (2010), "Exposed column base connections subjected to axial compression and flexure", AISC, Chicago, IL, USA.

Kanvinde, A.M., Grilli, D.A. and Zareian, F. (2012), "Rotational stiffness of exposed column base connections: experiments and analytical models", *J. Struct. Eng.*, **138**(5), 549-560. https://doi.org/10.1061/(ASCE)ST.1943-541X.0000495

Kanvinde, A.M., Jordan, S.J. and Cooke, R.J. (2013), "Exposed column base plate connections in moment frames – simulations and behavioral insights", *J. Constr. Steel. Res.*, **84**, 82-93. https://doi.org/10.1016/j.jcsr.2013.02.015

Kanvinde, A.M., Higgins, P., Cooke, R.J., Perez, J. and Higgins, J. (2015), "Column base connections for hollow steel sections: seismic performance and strength models", *J. Struct. Eng.*, **141**(7), 04014171. https://doi.org/10.1061/(ASCE)ST.1943-541X.0001136

Khodaie, S., Mohamadi-shooreh, M.R. and Mofid, M. (2012), "Parametric analyses on the initial stiffness of the SHS column base plate connections using FEM", *Eng. Struct.*, **34**, 363-370. https://doi.org/10.1016/j.engstruct.2011.09.026

Latour, M. and Rizzano, G. (2013), "Full strength design of column base connections accounting for random material variability", *Eng. Struct.*, **48**, 458-471. https://doi.org/10.1016/j.engstruct.2012.09.026

Latour, M., Piluso, V. and Rizzano, G. (2014), "Rotational behaviour of column base plate connections: Experimental analysis and modelling", *Eng. Struct.*, **68**, 14-23. https://doi.org/10.1016/j.engstruct.2014.02.037

Li, D.X., Uy, B., Aslani, F. and Patel, V. (2016), "Analysis and design of demountable steel column-baseplate connections", *Steel Compos. Struct., Int. J.*, **22**(4), 753-775. https://doi.org/10.12989/scs.2016.22.4.753

Li, D.X., Uy, B., Patel, V. and Aslani, F. (2017), "Analysis and design of demountable embedded steel column base connections", *Steel Compos. Struct., Int. J.*, **23**(3), 303-315. https://doi.org/10.12989/scs.2017.23.3.303

Nagae, T., Ikenage, M., Nakashima, M. and Suita, K. (2006), "Shear friction between base plate and base mortar in exposed steel column base", *J. Struct. Construct. Eng., Architect. Inst. Japan*, **606**, 217-223. https://doi.org/10.3130/aijs.71.217

Rodas, P.T., Zareian, F. and Kanvinde, A.M. (2016), "Hysteretic model for exposed column-base connections", *J. Struct. Eng.*, **142**(12), 04016137. https://doi.org/10.1061/(ASCE)ST.1943-541X.0001602

Sato, K. (1987), "A research on the aseismic behavior of steel column base for evaluating its strength capacity and fixity", Report No. 69; Kajima Institute of Construction Technology, Tokyo, Japan.

Stamatoloulos, G.N. and Ermopoulos, J.C. (2011), "Experimental and analytical investigation of steel column bases", *J. Constr. Steel. Res.*, **67**(9), 1341-1357. https://doi.org/10.1016/j.jcsr.2011.03.007

Thambiratnam, D.P. and Paramasivam, P. (1986), "Base plate under axial loads and moments", *J. Struct. Eng.*, **112**(5), 1166-1181. https://doi.org/10.1061/(ASCE)0733-9445(1986)112:5(1166)

DL

Notation

The following symbols are used in this paper

d	=	depth of column section
B	=	width of base plate
D	=	length of base plate
l	=	base plate edge distance
s	=	anchor rod edge distance
t_{bp}	=	thickness of base plate
T_{ya}	=	yield tensile force of the anchor rod
T_y	=	total yield tensile force of anchor rods on the tension side
θ_t	=	rotation of base plate on the tension side
θ_c	=	rotation of base plate on the compression side
θ	=	rotation of column
n	=	number of anchor rods in tension
A_e	=	effective area of anchor rod
$f_{y,ab}$	=	yield strength of anchor rods
$f_{y,bp}$	=	yield strength of base plate
σ_c	=	compressive strength of mortar layer per unit width
f_c	=	bearing stresses in mortar layer
M_{ab}	=	moment resistance caused by the elongation of anchor rods to the edge of steel column
$M_{bp,t}$	=	full plastic moment of a single yield line in the base plate on the tension side
$M_{bp,t}^{total}$	=	total full plastic moment resistance of yield lines in the base plate on the tension side
$M_{bp,c}$	=	full plastic moment of yield lines in the base plate on the compression side
M_b	=	moment of the base plate under the upward bearing stress on the compression side
$M_{y,B}$	=	yield moment resistance of exposed column base with flexible base plate
$M_{y,A}$	=	yield moment resistance of exposed column base with rigid base plate